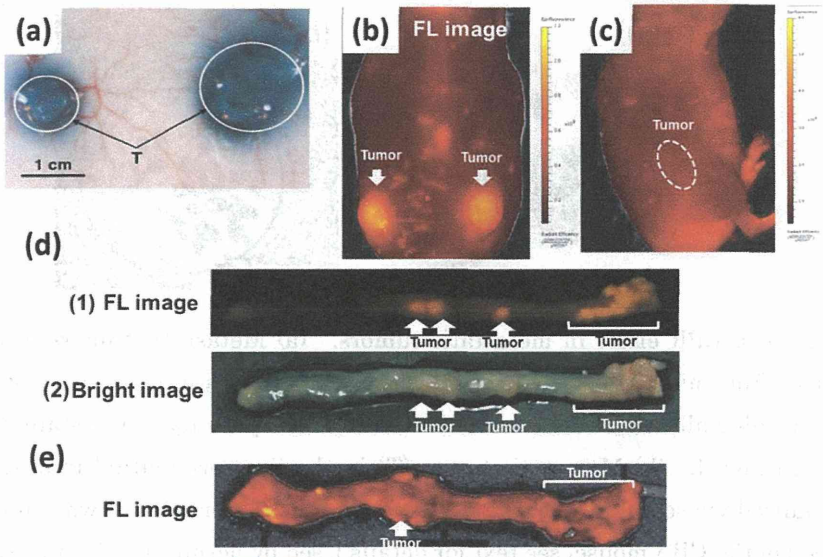

Figure 1. Visualization of the EPR effect. (a) Selective accumulation of the putative macromolecular drug complex Evans blue-albumin in a mouse S180 tumor (T) implanted bilaterally in the dorsal skin. (b) Fluorescent image of PHPMA-ZnPP. (c) Free ZnPP in the S180 implanted tumor model. The fluorescent image obtained 5 h after i.v. administration via IVIS Lumina XR shows no tumor-selective accumulation. (d) (1) Fluorescent (FL) image of autochthonous colon cancer from a mouse after using bovine serum albumin-conjugated rhodamine. The tumor was induced by azoxymethane and dextran sodium sulfate. The image was obtained 24 h after i.v. drug administration via a standard digital camera equipped with bandpass filter. (2) The normal light image, of the same colon sample as that seen in (1), shows no distinct tumor. (e) Fluorescent image of colon cancer (same as above) 5 h after i.v. injection of Lasephyrin. The image, obtained via IVIS Lumina XR, shows fluorescence that is not tumor-selective.

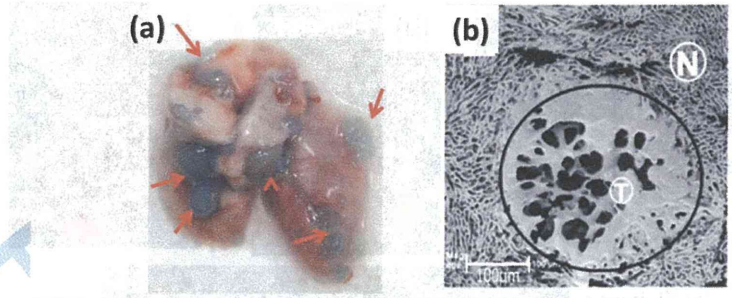

Figure 2 The EPR effect in metastatic tumors. (a) Metastatic tumors in the lung, originating from subcutaneously implanted colon 26 tumor, were visualized by staining with Evans blue-albumin. This result is similar to the primary tumor staining seen in Figure 1a and d. (b) Metastatic tumor (T) in the liver originating from the spleen was visualized via scanning electron microscopy. The tumor (MoCR) was implanted in the spleen of the CBA mouse; see text for details Used by permission from Daruwalla et al. [76].

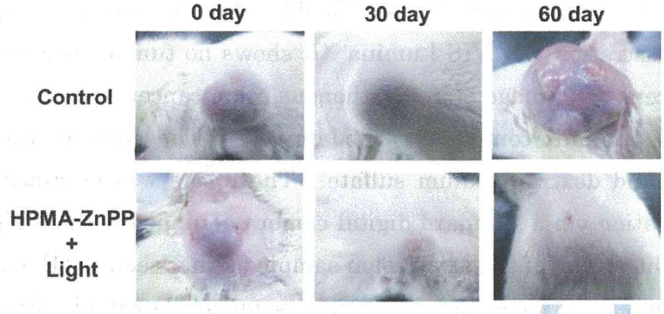

Figure 3 Photodynamic therapy in DMBA-induced breast cancer. A rat bearing the autochthonous breast tumor received no drug (control) or 15 mg/kg PHPMA-ZnPP i.v., and then tumors were irradiated with xenon light at 24 and 48 h after PHPMA-ZnPP administration and were observed at the times indicated. Complete tumor eradication was seen on day 60. The control is a similar tumor-bearing rat that did not receive ZnPP polymer but had the same dose of light irradiation. The control tumor continued to grow, as seen in human breast cancer.

Acknowledgement

We would like to acknowledge the financial supports of Research Grants from Government of Japan: Grant-in-Aids from MEXT, No.08011717 for HM, No.26860031 for HN, No.25430162 for JF, and Cancer Specialty Grant from MHWL, H23-3rd Cancer Project-General-001 for HM. Also, Ms. Judy Gandy for her excellent/invaluable assistance in English editing.

Declaration of interest

The authors state no conflict of interest and have received no payment of this manuscript.

References

1. DeVita VT Jr, Chu E. A history of cancer chemotherapy. Cancer Res 2008;68:8643-53.

2. Gilman A, Philips FS. The biological actions and therapeutic applications of the ß-chloroethyl amines and sulfides. Science 1946;103:409-36.

3. Macleod CM, Stone ER. Differences in the nature of antibacterial action of the sulfonamides and penicillin and their relation to therapy. Bull N Y Acad Med 1945;21:375-88.

4. Maeda H, Takeshita J, Kanamaru R. A lipophilic derivative of neocarzinostatin. A polymer conjugation of an antitumor protein antibiotic. Int J Pept Protein Res 1979;14:81-7.

5. Sliwkowski MX, Mellman I. Antibody therapeutics in cancer. Science 2013;341:1192-8.

6. Druker BJ, Tamura S, Buchdunger E, et al. Effects of a selective inhibitor of the Abl tyrosine kinase on the growth of Bcr-Abl positive cells. Nat Med 1996;2:561-6.

7. Deininger MW, Goldman JM, Lydon N, et al. The tyrosine kinase inhibitor CGP57148B selectively inhibits the growth of BCR-ABL-positive cells. Blood 1997;90:3691-8.

8. Kantarjian HM, Fojo T, Mathisen M, et al. Cancer drugs in the United States: *Justum Pretium*—the just price. J Clin Oncol 2013;31:3600-4.

9. Mohamed A, Krajewski K, Cakar B, et al. Targeted therapy for breast cancer. Am J Pathol 2013;183:1096-112.

10. Huang M, Shen A, Ding J, et al. Molecularly targeted cancer therapy: some lessons from the past decade. Trends Pharmacol Sci 2014;35:41-50.

11. Ricciardi S, Tomao S, de Marinis F. Toxicity of targeted therapy in non-small-cell lung cancer management. Clin Lung Cancer 2009;10:28-35.

12. Weber J. Review: anti-CTLA-4 antibody ipilimumab: case studies of clinical response and immune-related adverse events. Oncologist 2007;12:864-72.

13. McDermott DF, Atkins MB. PD-1 as a potential target in cancer therapy. Cancer Med 2013;2:662-73.

14. Vogelstein B, Papadopoulos N, Velculescu VE, et al. Cancer genome landscapes. Science 2013;339:1546-58.

15. Vogelstein B, Kinzler KW. Cancer genes and the pathways they control. Nat Med 2004;10:789-99.

16. Maeda H. Vascular permeability in cancer and infection as related to macromolecular drug delivery, with emphasis on the EPR effect for tumor-selective drug targeting. Proc Jpn Acad Ser B Phys Biol Sci 2012;88:53-71.

17. Noguchi Y, Wu J, Duncan R, et al. Early phase tumor accumulation of macromolecules: a great difference in clearance rate between tumor and normal tissues. Jpn J Cancer Res 1998;89:307-14.

18. Lammers T, Kiessling F, Hennink WE, et al. Drug targeting to tumors: principles, pitfalls and (pre-) clinical progress. J Control Release 2012;161:175-87.

19. Maeda H. The link between infection and cancer: tumor vasculature, free radicals, and drug delivery to tumors via the EPR effect. Cancer Sci 2013;104:779-89.

20. Maeda H, Fang J, Inutsuka T, et al. Vascular permeability enhancement in solid tumor: various factors, mechanisms involved and its implications. Int Immunopharmacol 2003;3:319-28.

21. Matsumura Y, Maeda H. A new concept for macromolecular therapeutics in cancer chemotherapy: mechanism of tumoritropic accumulation of proteins and the antitumor agent smancs. Cancer Res 1986;46:6387-92.

22. Maeda H. SMANCS and polymer-conjugated macromolecular drugs: advantages in cancer chemotherapy. Adv Drug Deliv Rev 2001;46:169-85.

23. Yuan F, Dellian M, Fukumura D, et al. Vascular permeability in a human tumor xenograft: molecular size dependence and cutoff size. Cancer Res 1995;55:3752-6.

24. Hashizume H, Baluk P, Morikawa S, et al. Openings between defective endothelial cells explain tumor vessel leakiness. Am J Pathol 2000;156:1363-80.

25. Iwai K, Maeda H, Konno T. Use of oily contrast medium for selective drug targeting to tumor: enhanced therapeutic effect and X-ray image. Cancer Res 1984;44:2115-21.

26. Konno T, Maeda H, Iwai K, et al. Selective targeting of anti-cancer drug and simultaneous image enhancement in solid tumors by arterially administered lipid contrast medium. Cancer 1984;54:2367-74.

27. Konno T, Maeda H, Iwai K, et al. Effect of arterial administration of high-molecular-weight anticancer agent SMANCS with lipid lymphographic agent on hepatoma: a preliminary report. Eur J Cancer Clin Oncol 1983;19:1053-65.

28. Maki S, Konno T, Maeda H. Image enhancement in computerized tomography for sensitive diagnosis of liver cancer and semiquantitation of tumor selective drug targeting with oily contrast medium. Cancer 1985;56:751-7.

29. Nagamitsu A, Greish K, Maeda H. Elevating blood pressure as a strategy to increase tumor-targeted delivery of macromolecular drug SMANCS: cases of advanced solid tumors. Jpn J Clin Oncol 2009;39:756-66.

30. Peterson HI, Appelgren KL. Experimental studies on the uptake and rentention of labelled proteins in a rat tumour. Eur J Cancer 1973;9:543-7.

31. Choi HS, Liu W, Misra P, et al. Renal clearance of quantum dots. Nat Biotechnol

2007;25:1165-70.

32. Kobayashi H, Brechbiel MW. Dendrimer-based macromolecular MRI contrast agents: characteristics and application. Mol Imaging 2003;2:1-10.

33. Maeda H, Matsumura Y, Oda T, et al. Cancer selective macromolecular therapeutics: tailoring of an antitumor protein drug. In Protein Tailoring for Food and Medical Uses (eds Feeney RE, Whitaker JR). New York and Basel: Marcel Dekker, 1986, pp 353-382.

34. Gabizon A, Catane R, Uziely B, et al. Prolonged circulation time and enhanced accumulation in malignant exudates of doxorubicin encapsulated in polyethylene-glycol coated liposomes. Cancer Res 1994;54:987-92.

35. Wolinsky JB, Colson YL, Grinstaff MW. Local drug delivery strategies for cancer treatment: gels, nanoparticles, polymeric films, rods, and wafers. J Control Release 2012;159:14-26.

36. Knop K, Hoogenboom R, Fischer D, et al. Poly(ethylene glycol) in drug delivery: pros and cons as well as potential alternatives. Angew Chem Int Ed Engl 2010;49:6288-308.

37. Bala I, Hariharan S, Kumar MN. PLGA nanoparticles in drug delivery: the state of the art. Crit Rev Ther Drug Carrier Syst 2004;21:387-422.

38. Mishra B, Patel BB, Tiwari S. Colloidal nanocarriers: a review on formulation technology, types and applications toward targeted drug delivery. Nanomedicine 2010;6:9-24.

39. Lammers T. Improving the efficacy of combined modality anticancer therapy using HPMA copolymer-based nanomedicine formulations. Adv Drug Deliv Rev 2010;62:203-30.

40. van Etten EW, ten Kate MT, Stearne LE, et al. Amphotericin B liposomes with prolonged circulation in blood: in vitro antifungal activity, toxicity, and efficacy in systemic candidiasis in leukopenic mice. Antimicrob Agents Chemother 1995;39:1954-8.

41. Gabizon AA, Barenholz Y, Bialer M. Prolongation of the circulation time of doxorubicin encapsulated in liposomes containing a polyethylene glycol-derivatized phospholipid: pharmacokinetic studies in rodents and dogs. Pharm Res 1993;10:703-8.

42. Fechtenbaum M, Md Yusof MY, Emery P. Certolizumab pegol in rheumatoid arthritis: current update. Expert Opin Biol Ther 2014: posted online 22 March 2014, doi:10.1517/14712598.2014.900043

43. Shannon JA, Cole SW. Pegloticase: a novel agent for treatment-refractory gout. Ann Pharmacother 2012;46:368-76.

44. He C, Hu Y, Yin L, et al. Effects of particle size and surface charge on cellular uptake and biodistribution of polymeric nanoparticles. Biomaterials 2010;31:3657-66.

45. Brown LF, Dvorak AM, Dvorak HF. Leaky vessels, fibrin deposition, and fibrosis: a

sequence of events common to solid tumors and to many other types of disease. Am Rev Respir Dis 1989;140:1104-7.

46. Hori K, Suzuki M, Saito S, et al. Changes in vessel pressure and interstitial fluid pressure of normal subcutis and subcutaneous tumor in rats due to angiotensin II. Microvasc Res 1994;48:246-56.

47. Skinner SA, Tutton PJ, O'Brien PE. Microvascular architecture of experimental colon tumors in the rat. Cancer Res 1990;50:2411-7.

48. Abe I, Hori K, Saito S, et al. Increased intratumor concentration of fluorescein-isothiocyanate-labeled neocarzinostatin in rats under angiotensin-induced hypertension. Jpn J Cancer Res 1988;79:874-9.

49. Suzuki M, Hori K, Abe I, et al. A new approach to cancer chemotherapy: selective enhancement of tumor blood flow with angiotensin II. J Natl Cancer Inst 1981;67:663-9.

50. Li CJ, Miyamoto Y, Kojima Y, et al. Augmentation of tumour delivery of macromolecular drugs with reduced bone marrow delivery by elevating blood pressure. Br J Cancer 1993;67:975-80.

51. Wu J, Akaike T, Maeda H. Modulation of enhanced vascular permeability in tumors by a bradykinin antagonist, a cyclooxygenase inhibitor, and a nitric oxide scavenger. Cancer Res 1998;58:159-65.

52. Marketou ME, Vardas PE. Bradykinin in the treatment of arterial hypertension: friend or foe? Hellenic J Cardiol 2012;53:91-4.

53. Noguchi A, Takahashi T, Yamaguchi T, et al. Enhanced tumor localization of monoclonal antibody by treatment with kininase II inhibitor and angiotensin II. Jpn J Cancer Res 1992;83:240-3.

54. Seki T, Fang J, Maeda H. Enhanced delivery of macromolecular antitumor drugs to tumors by nitroglycerin application. Cancer Sci 2009;100:2426-30.

55. Yasuda H. Solid tumor physiology and hypoxia-induced chemo/radio-resistance: novel strategy for cancer therapy: nitric oxide donor as a therapeutic enhancer. Nitric Oxide 2008;19:205-16.

56. Janssens MY, Van den Berge DL, Verovski VN, et al. Activation of inducible nitric oxide synthase results in nitric oxide-mediated radiosensitization of hypoxic EMT-6 tumor cells. Cancer Res 1998;58:5646-8.

57. Yasuda H, Yamaya M, Nakayama K, et al. Randomized phase II trial comparing nitroglycerin plus vinorelbine and cisplatin with vinorelbine and cisplatin alone in previously untreated stage IIIB/IV non-small-cell lung cancer. J Clin Oncol 2006;24:688-94.

58. Estrada C, Gomez C, Martin C, et al. Nitric oxide mediates tumor necrosis factor-α cytotoxicity in endothelial cells. Biochem Biophys Res Commun 1992;186:475-82.

59. Brett J, Gerlach H, Nawroth P, et al. Tumor necrosis factor/cachectin increases permeability of endothelial cell monolayers by a mechanism involving regulatory G proteins. J Exp Med 1989;169:1977-91.

60. Ferrero E, Villa A, Ferrero ME, et al. Tumor necrosis factor α-induced vascular leakage involves PECAM1 phosphorylation. Cancer Res 1996;56:3211-5.

61. Eggermont AM, Schraffordt Koops H, et al. Isolated limb perfusion with tumor necrosis factor and melphalan for limb salvage in 186 patients with locally advanced soft tissue extremity sarcomas. The cumulative multicenter European experience. Ann Surg 1996;224:756-64; discussion 64-5.

62. Seki T, Carroll F, Illingworth S, et al. Tumour necrosis factor-alpha increases extravasation of virus particles into tumour tissue by activating the Rho A/Rho kinase pathway. J Control Release 2011;156:381-9.

63. Failli P, Vannacci A, Di Cesare Mannelli L, et al. Relaxant effect of a water soluble carbon monoxide-releasing molecule (CORM-3) on spontaneously hypertensive rat aortas. Cardiovasc Drugs Ther 2012;26:285-92.

64. Motterlini R, Sawle P, Hammad J, et al. Vasorelaxing effects and inhibition of nitric oxide in macrophages by new iron-containing carbon monoxide-releasing molecules (CO-RMs). Pharmacol Res 2013;68:108-17.

65. Abraham NG, Kappas A. Pharmacological and clinical aspects of heme oxygenase. Pharmacol Rev 2008;60:79-127.

66. Leffler CW, Parfenova H, Jaggar JH. Carbon monoxide as an endogenous vascular modulator. Am J Physiol Heart Circ Physiol 2011;301:H1-H11.

67. Fang J, Akaike T, Maeda H. Antiapoptotic role of heme oxygenase (HO) and the potential of HO as a target in anticancer treatment. Apoptosis 2004;9:27-35.

68. Jozkowicz A, Was H, Dulak J. Heme oxygenase-1 in tumors: is it a false friend? Antioxid Redox Signal 2007;9:2099-117.

69. Murphy BJ, Laderoute KR, Vreman HJ, et al. Enhancement of heme oxygenase expression and activity in A431 squamous carcinoma multicellular tumor spheroids. Cancer Res 1993;53:2700-3.

70. Fang J, Qin H, Nakamura H, et al. Carbon monoxide, generated by heme oxygenase-1, mediates the enhanced permeability and retention effect in solid tumors. Cancer Sci 2012;103:535-41.

71. Barth G, Huth E, Wachsmann F. [Experimental investigations on hyperthermia therapy of neoplasms]. Strahlentherapie 1952;88:1-7.

72. Kong G, Braun RD, Dewhirst MW. Hyperthermia enables tumor-specific nanoparticle delivery: effect of particle size. Cancer Res 2000;60:4440-5.

73. Kong G, Braun RD, Dewhirst MW. Characterization of the effect of hyperthermia on nanoparticle extravasation from tumor vasculature. Cancer Res 2001;61:3027-32.

74. Buckway B, Frazier N, Gormley AJ, et al. Gold nanorod-mediated hyperthermia enhances the efficacy of HPMA copolymer-(90)Y conjugates in treatment of prostate tumors. Nucl Med Biol 2014;41:282-9.

75. Lammers T. Drug delivery research in Europe. J Control Release 2012;161:151.

76. Daruwalla J, Nikfarjam M, Greish K, et al. In vitro and in vivo evaluation of tumor targeting styrene-maleic acid copolymer-pirarubicin micelles: survival improvement and inhibition of liver metastases. Cancer Sci 2010;101:1866-74.

77. Northfelt DW, Martin FJ, Working P, et al. Doxorubicin encapsulated in liposomes containing surface-bound polyethylene glycol: pharmacokinetics, tumor localization, and safety in patients with AIDS-related Kaposi's sarcoma. J Clin Pharmacol 1996;36:55-63.

78. Maeda H. Macromolecular therapeutics in cancer treatment: the EPR effect and beyond. J Control Release 2012;164:138-44.

Improved pharmacokinetics and antitumor activity of new dendrimer-derived poly(*N*-(2-hydroxypropyl)methacrylamide) conjugates of pirarubicin

Hideaki Nakamura[a,b], Eva Koziolová[c], Tomas Etrych[c], Petr Chytil[c], Jun Fang[a,b], Karel Ulbrich[c], Hiroshi Maeda[a*]

[a]*Research Institute for Drug Delivery Science,* and [b]*Laboratory of Microbiology and Oncology, Faculty of Pharmaceutical Sciences, Sojo University, Ikeda 4-22-1, Nishi-ku, Kumamoto, 860-0082, Japan*
[c]*Institute of Macromolecular Chemistry, Academy of Sciences of the Czech Republic, Heyrovsky Sq. 2, 162 06 Prague 6, Czech Republic*

*Corresponding author: Institute for DDS, Sojo University, Ikeda 4-22-1, Nishi-ku, Kumamoto, Japan 860-0082. Tel.: +81-96-326-4114; fax: +81-96-326-3185. E-mail address: hirmaeda@ph.sojo-u.ac.jp (H. Maeda).

Keywords: HPMA polymer conjugate, pirarubicin (THP), acid-cleavable linkage, EPR effect, dendrimer conjugated THP

Abbreviations: THP: 4'-O-tetrahydropyranyl doxorubicin; DOX: doxorubicin; SP: star polymer; LP: linear polymer; AUC: area under the curve; AOM: azoxymethan; DSS: dextran sodium sulfate; HPMA: *N*-(2-hydroxyproyl)methacrylamide; EPR: enhanced permeability and retention; PEG: polyethylene glycol; PAMAM: polyamido amine; ABIC: 4,4′-azobis(4-cyanovaleric acid); DIPC: *N,N′*-diisopropylcarbodiimide; EDPA: *N*-ethyldiisopropylamine; TNBSA: 2,4,6-trinitrobenzene-1-sulfonic acid; MTT: 3-(4,5-Dimethyl-2-thiazolyl)-2,5-diphenyl-2H-tetrazolium bromide

Novelty and impact of the work.

This article describes comparison of two different types of antitumor polymer-conjugated drugs; LP (linear polymer)-THP and SP (spherical polymer, dendrimer)-THP conjugates, respectively, and clarified tissue distribution, therapeutic efficacy, and toxicity. Excellent tumor selective accumulation was observed after i.v. administration of both polymeric drug-conjugates. Both showed far superior therapeutic effect, and least toxicity, than parental low MW free THP (pirarubicin). Especially, SP-THP showed remarkable therapeutic efficacy against not only implanted tumor model but also chemical- induced autochthonous tumor in the colon, which warrant further development.

Abstract

Previously we showed that linear poly(*N*-(2-hydroxypropyl)methacrylamide) conjugates of pirarubicin (THP), LP-THP, with MW about 39 kDa, exhibited far better tumor accumulation and therapeutic effect than that of parental free THP. To improve the pharmacokinetics of LP-THP further, high-MW conjugate of poly(amido amine) (PAMAM) dendrimer grafted with semitelechelic HPMA copolymer (PHPMA) was synthesized [star polymer (SP); 400 kDa] and conjugated with THP via hydrazone bond-containing spacer (SP-THP). Here we describe the synthesis of the SP-THP conjugate and evaluation of its antitumor action in *in vitro* and *in vivo* system. SP-THP consists of 2nd generation dendrimer in the core, of which surface amino groups were grafted with LP-THP. THP was conjugated to SP to form SP-THP via acid cleavable hydrazone bonding, which responds to acidic milieu of tumor tissue. As a consequence, it would release free THP, by active therapeutic principle, at the lysosomes and endosomes of tumor cells. SP-THP exhibits larger hydrodynamic diameter (25.9 nm) in aqueous solution than that of LP-THP (8.6 nm) as observed by light scattering and size exclusion chromatography. Because of the larger size, the tumor $AUC_{5h\text{-}72h}$ of SP-THP was 3.3 times higher than that of LP-THP. More importantly, released free THP was retained selectively in the tumor tissue for at least up to 72h after administration of SP-THP. Tumor level of THP was 10 – 30 times higher than in the normal tissue, resulting in much lower side effect compared to conventional free THP. In *in vivo* antitumor study, S-180 tumor-bearing mice, and chemically with AOM / DSS-induced colon tumor-bearing mice were used to compare the therapeutic efficacy of SP-THP and LP-THP. SP-THP exhibited superior antitumor effect to LP-THP against both S-180 and AOM / DSS-induced colon tumor.

Introduction

4'-O-tetrahydropyranyl doxorubicin (Pirarubicin®, or THP) is an anthracycline antibiotic used for treatment of various cancers in such organs as breast, head and neck, cervix, and lymphoma, etc [1]. An intrinsic problem of low-MW anticancer drugs is also applicable to THP (MW 628); its body distribution is indiscriminate in all normal tissues and organs before tumor delivery. Thus adverse effects such as bone-marrow suppression, cardiac toxicity as well as others limit the usage of higher dose of THP in clinical setting. Thus improvement of pharmacokinetics, especially tumor selective delivery is the prime requirement.

Poly(*N*-(2-hydroxypropyl)methacrylamide (PHPMA) is highly water-soluble biocompatible macromolecule, namely nontoxic and non-immunogenic. [2, 3]. After intravenous injection, high-MW PHPMA (more than 40 kDa) is retained in the systemic circulation for longer time (> 24h) at significant concentration, thus it preferentially accumulates in the tumor tissue by enhanced permeability and retention (EPR) effect [4]. By conjugating low-MW antitumor drugs to the PHPMA, the tumor accumulation of the antitumor drug can be enhanced and the therapeutic response for solid tumor improved.

To improve the tumor accumulation of PHPMA drug conjugates, molecular size of PHPMA may be increased; either by branching or grafting HPMA copolymers or by their self-assembly to form high-MW micellar structures. However, the synthesis of explicitly branched side chains or graft polymers in comb structure is relatively difficult to control; high polydispersity index and lower reproducibility become a concern. On the other hand, dendrimer is nearly monodisperse, and its surface can be freely and explicitly modified, e.g. by attaching semitelechelic

PHPMA. Grafting of the dendrimer by PHPMA decreases the toxicity of the dendrimer as well. Along this line, we previously reported that star-like HPMA copolymer, PHPMA-modified PAMAM dendrimer (SP-THP) conjugated with doxorubicin (DOX), showed superior tumor accumulation, and also antitumor activity to that of linear HPMA copolymer conjugates of DOX [5, 6]. Although previous star polymer-DOX conjugate showed high effectivity *in vivo*, a problem was that free DOX liberated from the conjugate exhibited slow intracellular uptake into tumor cells compared to free THP. Namely, it required about 100 times slower uptake time, probably it only depended on free diffusion mechanism. Consequently, slow uptake by tumor cells would result in wash out from the tumor site back into systemic circulation, followed by excretion from the body. Therefore, THP polymer conjugate would offer more advantage in *in vivo* setting, but not as much in *in vitro* culture cell system, and thus we have undertaken the present study.

In these polymer conjugates we utilized biodegradable linkers to attach the drug to the polymer [7, 8]. Advantage of using biodegradable linker is that the drug can be released from the polymer at or near the pathological region and then exhibits better therapeutic effect. One problem is connected with the use of some highly biocompatible polymer conjugates such as PEG or HPMA copolymer-conjugated drugs. They have lower intracellular uptake velocity than free drug, and consequently lower interaction with the target molecules resulting in lower therapeutic effect than one could expect [9-11]. Therefore, good release of low-MW drugs from the conjugates at tumor site is a critical issue for achieving the superior therapeutic effect, in order to exert drug action to the tumor [9]. For conjugating low-MW drugs, peptide, ester, disulfide and hydrazone bonds were used for conjugating the polymer and drugs [12, 13]. These chemical bonds can be cleaved by proteases and esterases which exist more dominantly in the tumor tissue. In addition, more acidic pH favors the spontaneous cleavage of hydrazone bond. Therefore, we designed conjugates with pH-controlled drug release taking place preferencially at the tumor tissue and at pathological lesions.

Here we describe the synthesis of SP-THP designed for efficient tumor accumulation due to the EPR effect of its macromolecular nature and we present results of the biological evaluation of novel dendrimer attached (star-like PHPMA copolymer conjugate of THP (SP-THP), in which surface of 2nd generation PAMAM (polyamido amine) dendrimer was grafted with chains of HPMA copolymers, which are conjugated with THP. For the detailed chemical structure of HPMA copolymer THP conjugate see [17]. THP was conjugated to the PHPMA via hydrazone bond, thus efficient drug release occur in the acidic environment of lysosomal pH and/or of tumor tissue. When we compared antitumor activity of SP-THP conjugate with linear HPMA copolymer-THP conjugate (LP-THP using two types of mouse tumor models, implanted and chemically induced tumor, we found superior tumor accumulation of SP-THP, and thus better therapeutic effect.

Materials and Methods

Materials

1-Aminopropan-2-ol, methacryloyl chloride, 4,4′-azobis(4-cyanovaleric acid) (ABIC), 6-aminohexanoic acid (ah), *N,N′*-dimethylformamide (DMF), *N,N′*-diisopropylcarbodiimide (DIPC), *N*-ethyldiisopropylamine (EDPA), dimethyl sulfoxide (DMSO), *tert*-butyl carbazate, trifluoroacetic acid (TFA) and 2,4,6-trinitrobenzene-1-sulfonic acid (TNBSA) were purchased from Sigma-Aldrich. Pirarubicin was purchased from Abbliss Chemicals, Houston, USA and poly(amido amine)

(PAMAM) dendrimers with 1,4-diaminobutane core were purchased from Dendritic Nanotechnologies, Inc., Atlanta, USA. Male ddY mice and ICR mice were purchased from Kyudo Co., Ltd, Saga, Japan. Dulbecco-MEM (DMEM) was purchased from Nissui Seiyaku, Tokyo, Japan. Azoxymethane, dextran sodium sulfate, and reagent grade salts were purchased from Wako Pure Chemical Industry, Osaka, Japan. 3-(4,5-Dimethyl-2-thiazolyl)-2,5-diphenyl-2H-tetrazolium bromide (MTT) was purchased from Dojindo Chemical Laboratories, Kumamoto, Japan. Fetal calf serum was purchased from Nichirei Bioscience, Tokyo, Japan.

Synthesis of monomers

***N*-(2-Hydroxypropyl)methacrylamide** (HPMA) was synthesized as described in [14] using K_2CO_3 as a base. m.p. 70 °C; purity > 99.8 % (HPLC); elemental analysis: calc., C 58.72 %, H 9.15 %, N 9.78 %; found, C 58.98 %, H 9.18 %, N 9.82 %.

***N*-(*tert*-Butoxycarbonyl)-*N'*-(6-methacrylamidohexanoyl)hydrazine** (Ma-ah-NHNH-Boc) was prepared in two-step synthesis as described in [15]. M.p. 110-114 °C; purity (HPLC) > 99.5 %; elemental analysis: calcd. C 57.70 C, H 8.33, N 13.46; found C 57.96, H 8.64, N 13.25. Purity of both monomers mentioned above was examined by HPLC (Shimadzu, Japan) using a reverse-phase column Chromolith Performance RP-18e 100-4.6 with PDA detection, eluent water–acetonitril with acetonitril gradient 0 – 100 vol.%, flow rate, 0.5 mL/min, and ^{1}H NMR Bruker spectrometer (300 MHz).

Synthesis of star-like polymer precursor

The star polymer precursor was prepared by grafting PHPMA with terminal thiazolidine-2-thione (TT) chain end group onto the 2nd generation PAMAM dendrimers containing terminal amino groups as described recently [16]. Briefly: Poly(HPMA-co-Ma-ah-NHNH-Boc) terminated with TT group **(copolymer I)** was prepared by radical solution copolymerization in DMSO initiated with azo-initiator ABIC-TT. Consequently, the star-like polymer precursor (Mw 256 000, In 2.1) was prepared by grafting the semitelechelic **copolymer I** onto PAMAM dendrimer (aminolysis of the copolymer TT group with amino groups of PAMAM in methanol). After 2 h, low-MW impurities were removed by gel filtration (Sephadex LH-20, solvent methanol) and the star hydrazide groups-containing polymer precursor (**copolymer II**) was isolated, after deprotection of the Boc protecting groups with concentrated TFA, by precipitation in ethyl acetate.

Synthesis of star polymer conjugate

The star polymer conjugate with pirarubicin attached via a pH-sensitive hydrazone bond was prepared by the reaction of the hydrazide groups-containing **copolymer II** with pirarubicin in methanol in the dark. After 18 h the conversion reached 98% (determined by HPLC in methanol/aqueous buffer solvent as described below) and the star polymer-drug conjugate was purified from low-Mw impurities (pirarubicin or its degradation products) by precipitation into ethylacetate. M_w = 400,000 g/mol; I_n = 2.3, content of THP = 10.9 %wt; R_h= 13 nm. LP-THP was synthesised as describe before [17].

Cytotoxicity assay

HeLa cells (human cervical carcinoma) or B16-F10 cells (mouse melanoma) were maintained in DMEM supplemented with 10% fetal calf serum with 5% CO_2/air at 37 °C. HeLa cells were then incubated with SP-THP or LP-THP, or free THP for 72 h. The MTT assay was performed to quantify the cytotoxicity, with absorbance at 570 nm as usual.

Animal handling and evaluation of in vivo antitumor activity

The care and maintenance of animals were undertaken in accordance with the Institutional Animal Care and Use Committee of Sojo University.

S-180 tumor

Mouse sarcoma S-180 cells (2×10^6 cells) were implanted subcutaneously in the dorsal skin of ddY mice. When tumors became a diameter of about 4 mm, 5 or 15 mg/kg THP-equivalent drugs of SP-THP, LP-THP, or free THP in saline were injected intravenously (i.v.) at a volume of 0.2 mL per mouse. The tumor volume, body weight, and survival rate were recorded throughout the experiment period. The tumor volume (mm^3) was calculated as $(W^2 \times L)/2$ by measuring the length (L) and width (W) of the tumor on the dorsal skin.

AOM/DSS chemical induced colorectal tumor

Male ICR mice were administered i.p. injection of 10 mg/kg AOM (azoxymethan). One week after, mice were administered with 2% DSS p.o. for 1 week ad libitum. 10 weeks later, mice were randomly grouped, then 5 or 15 mg/kg THP-equivalent drugs in saline were injected i.v., 0.2 mL per mouse. Four weeks later, colon specimens were dissected, and number of tumor nodules and tumor area were calculated using ImageJ software.

Pharmacokinetics

S-180 tumor-bearing mice were administered 10 mg of THP equivalent/kg of LP-THP or SP-THP. At the indicated time periods, mice were killed, blood samples were withdrawn, and tissues were dissected after perfusion of the vascular void with physiological saline. Each tissue was homogenized by polytron homogenizer (Kinematica AG, Switzerland) after addition of PBS (900 μL/100 mg tissue). The amounts of total THP and released free THP in each tissue were measured as described previously [17].

Results

Physicochemical properties of SP-THP

SP-THP was synthesized as described in Materials and Methods. Apparent MW of each polymer conjugate was 400 kDa for SP-THP and 39 kDa for LP-THP respectively (Fig 1A). Loading of THP in SP-THP and LP-THP was 10.9 w/w % and 10.0 w/w % respectively. Hydrodynamic size of SP-THP in 10 mM phosphate buffered (pH 7.4) 0.15 M NaCl (PBS) was measured by dynamic light scattering, and found 25.9 ± 12.5 nm, which is larger than that of LP-THP (8.2 ± 1.7 nm) (Fig. 1B). Behavior of SP-THP in aqueous solution was also examined by size exclusion column chromatography on SB804-HQ column (SHODEX, tokyo). SP-THP was more quickly eluted than LP-THP, indicating that SP-THP behaved larger size molecule than LP-THP in aqueous solution (Fig. 1C).

Fig. 1

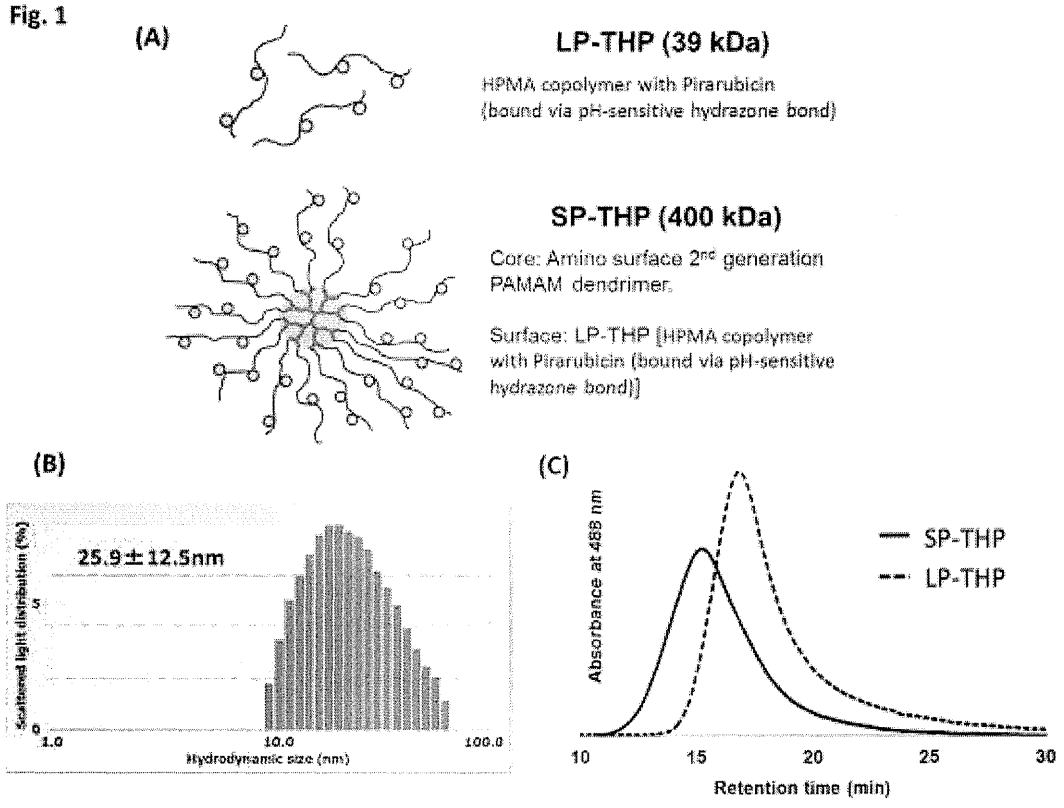

Fig. 1 Molecular size of SP-THP. (A) Illustrated image of LP-THP and SP-THP. (B) Hydrodynamic size of SP-THP dissolved in PBS at a concentration of 1 mg/mL was determined by dynamic light scattering (Otsuka Photal Electronics Co. Ltd., Osaka). (C) Size exclusion chromatography chromatograms of SP-THP and LP-THP using the column OHpak SB-804 HQ column (Showa Denko, Tokyo, Japan) (300 mm × 8.0 mm). Eluates were detected by photodiode array detector with absorbance at 488 nm.

Release of free THP

Cleavage of hydrazone bond, to release the free THP from SP-THP or LP-THP, was measured in aqueous solution in different pHs and we found that the release of THP from conjugates was pH dependent; 14 % was released in pH 7.4 and 88 % released in pH 5.0, both at 24h (Fig. 2). However, no significant difference in THP release was seen between SP-THP and LP-THP.

Fig. 2

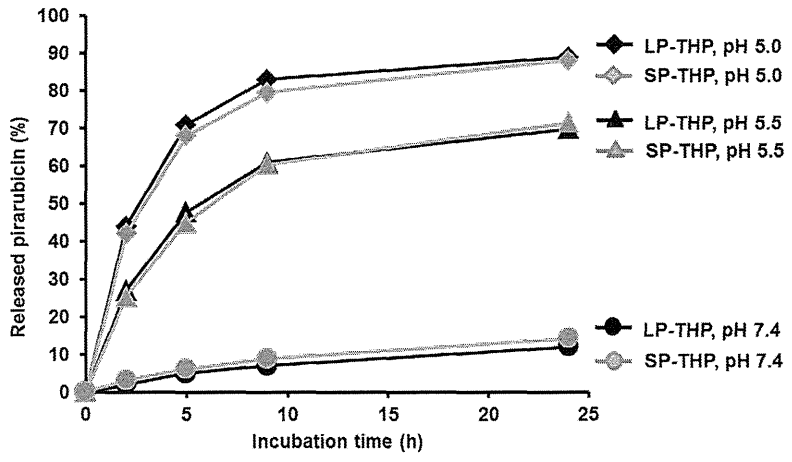

Fig. 2. Release of free THP from SP-THP and LP-THP. SP-THP and LP-THP was incubated in 0.1 M phosphate buffer (with 0.05 M NaCl) at pH 5.0, 5.5 or 7.4 at 37 °C. At indicated time period, released THP was determined by HPLC.

Cytotoxicity of polymer THP conjugates

Cytotoxicity of SP-THP was examined using HeLa and B16/F10 cells in vitro, and found to be dose dependent. The cytotoxicity was 5 – 10 times lower than that of free THP. IC_{50} values of free THP, SP-THP, and LP-THP against HeLa cells were 0.08, 0.53, and 0.61μg/mL respectively (Fig. 3A). No remarkable difference in cytotoxicity was seen between SP-THP and LP-THP against both cell lines, HeLa and B16/F10 (Fig.3A and B).

Fig. 3

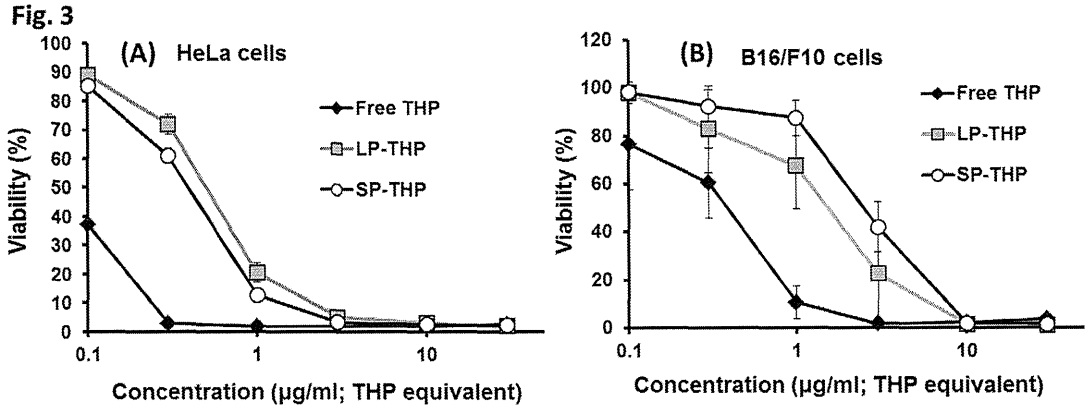

Fig. 3. Cytotoxicity of SP-THP and LP-THP. (A) HeLa, or (B) B16/F10 cells were treated with indicated concentration of SP-THP, LP-THP, or free THP for 72h, then viable cells were measured by MTT assay. Viablility (%) in comparison with the non-treated control group was calculated. Values are mean ± S.D. Cytotoxicity of LP-THP and free THP was adapted from [17].

Pharmacokinetics of polymer-THP conjugates

Body distribution of SP-THP was examined in S-180 sarcoma mouse model. Ten mg/kg THP equivalent of SP-THP was injected i.v. at indicated time period. The level of THP as total

amount of THP (which was SP-THP and released free THP combined) and released free THP in each tissue was examined. At earlier time point than 24 h after i.v. administration, the highest total THP concentration was found in the plasma, and followed by tumor and then other normal organs (Fig. 4A (a)). However, as time passed, total THP concentration in tumor was slightly increased by EPR effect, in contrast to the decreasing concentration in plasma and in other normal organs (Fig. 4A). More interestingly, concentration of released free THP continued to increase in tumor up to 48 h after i.v. administration of SP-THP (Fig. 4B); released free THP concentration in tumor tissue was highest compared with all other normal tissues after 24 h up to 72 h (Fig. 4B). Tumor accumulation of SP-THP was approx 3 times higher than that of LP-THP (Fig. 4C).

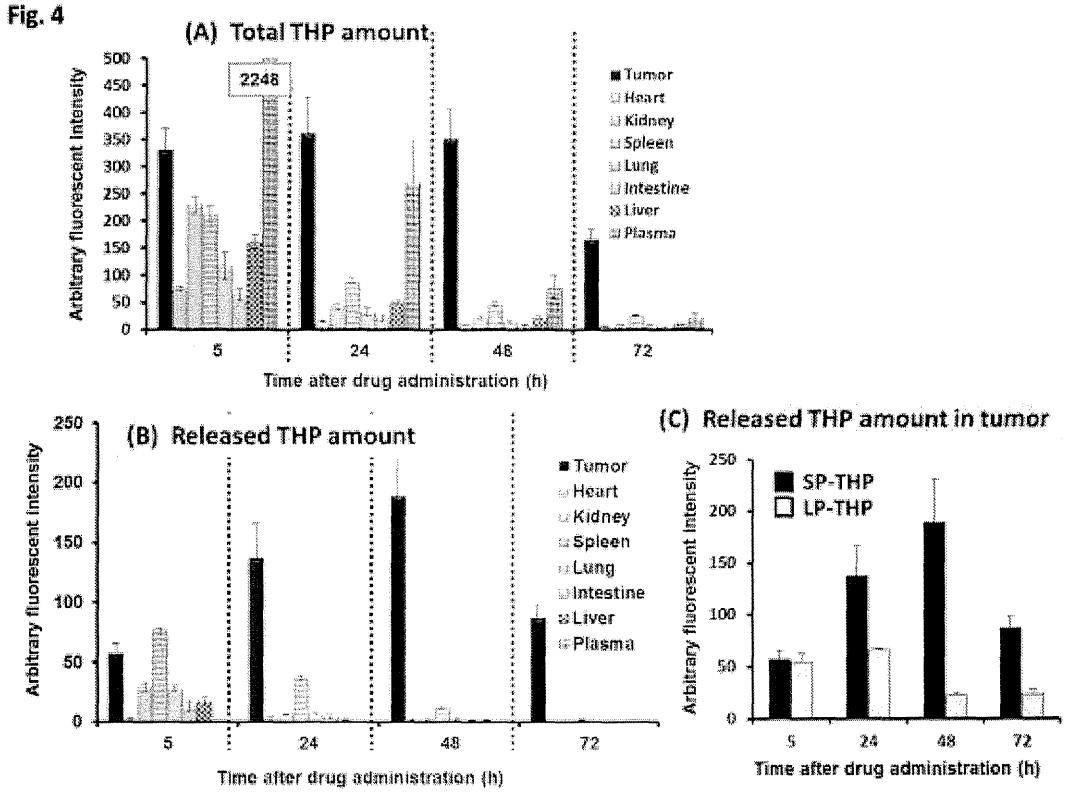

Fig. 4. Body distribution of SP-THP. (A) Amount of total THP (SP-THP + released THP), or (B) amount of released free THP in each tissues was detemined at indicated time intervals after drug admininistration. (C) Amount of released THP in the tumor after the treatment with SP-THP or LP-THP (Values are means ± S.E. (n=3))

In vivo antitumor activity in S-180 tumor model

In the next experiment we examined *in vivo* antitumor activity of SP-THP against mouse sarcoma S-180, ectopically implanted tumor model. THP equivalent dose of SP-THP at 5 mg/kg was intravenously administered. Tumor in the non-treated control group was continued to grow, whereas, injection of SP-THP only once completely suppressed the tumor growth. Tumor suppression lasted at least up to 80 days after tumor inoculation. In contrast to the SP-THP, administration of LP-THP i.v. could not suppress tumor growth completely; tumor of one mouse out of five mice grew (Fig. 5).

Apparent body weight loss was not observed, at a dose of 5 mg/kg, in both SP-THP and LP-THP treated groups.

Fig. 5

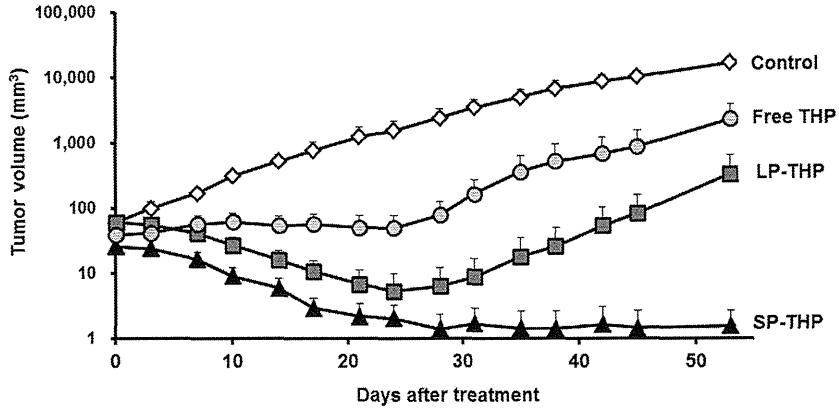

Fig. 5. *In vivo* antitumor effect against S-180 tumor model. S-180 tumor bearing mice with tumor size of 5 – 6 mm was administered at a 5 mg/kg THP equivalent dose of free THP, LP-THP, and SP-THP. Values are means ± S.E. (n = 5 ~ 6)

In vivo antitumor activity of SP-THP in chemical AOM/DSS induced tumor model

Chemically induced tumor is more realistic model to clinical tumor than ectopically implanted tumor, especially regarding orthotopicity and autochthonous nature. The antitumor effect of SP-THP against chemical AOM (azoxymethane) / DSS (dextran sodium sulfate) induced colon tumor model is shown in SFig.1. Though administration of free THP or LP-THP did not suppress the tumor growth (number of tumor nodule and tumor area), 15 mg/kg THP equivalent dose of SP-THP clearly suppressed the tumor number and size (Fig. 6A and 6B). Slight body weight loss was observed in SP-THP treated group; though ~ 15 % (SFig.2).

Fig. 6

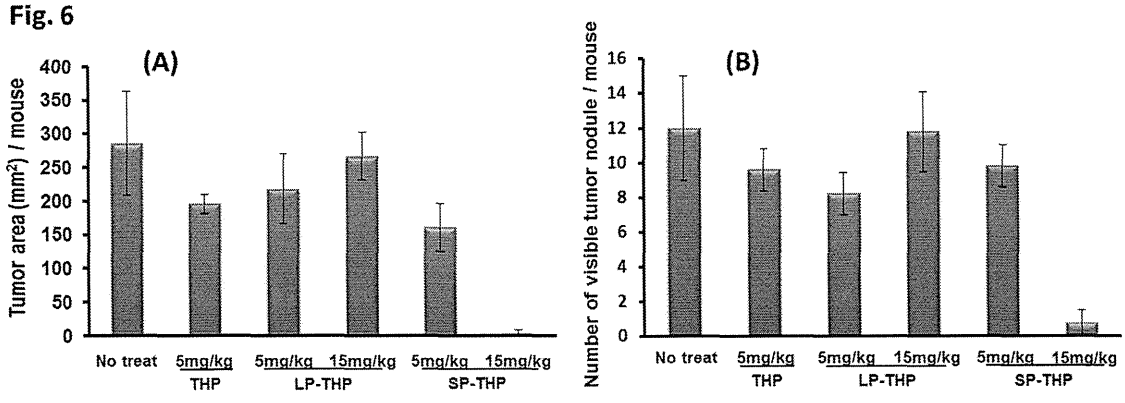

Fig. 6. *In vivo* antitumor activity of SP-THP in the AOM / DSS induced colon tumor model. AOM / DSS induced colon tumor bearing mice were adminstered at a 5 – 15 mg/kg THP equivalent dose of free THP, LP-THP, and SP-THP. Four weeks later after treatment, colons were dissected, and tumor area (A) and number of tumor nodules (B) was calculated by using of ImageJ software. Values are means ± S.E. (n=5)

Discussion

Importance of free drug release at the target tissue, and its tumor cell uptake for achieving superior therapeutic effect are discussed elsewhere [18-20]. Therefore, biodegradable linkers such as peptide, ester, disulfide, acetal, and hydrazone etc. have been introduced between polymer carrier and therapeutic drugs [12]. In this study, we utilized the hydrazone linkage, which could be cleaved at the slightly acidic condition of tumor tissue. Hydrazone bond can be cleaved at the interstitial space of tumor tissue and intracellularly in lysosomes, thus, selective release of drug at the tumor tissue can be anticipated [16, 17]. Acid pH-labile hydrazone bond is useful for selective tumor drug release, because released active drug is the primary agent to show the therapeutic effect. Release profile of free THP from polymer conjugates, SP-THP and LP-THP, was examined, and found to be almost the same for both conjugates(Fig. 2). Essentially, THP was covalently bound to fully solvated PHPMA chain in both SP-THP and LP-THP via the same linkage, thus net MW of polymer conjugate might not affect the sensitivity to the hydrolysis of the hydrazone linkage.

As regards to the cytotoxicity (Fig. 3) and intracellular uptake (data not shown) of polymer conjugates, there was no remarkable difference between SP-THP and LP-THP. Considering these results, biological activity of SP-THP and LP-THP was almost similar at least in *in vitro* assay.

So, what was difference between SP-THP and LP-THP? Remarkable difference was in MW of SP-THP (400 kDa) and LP-THP (39 kDa) (Fig 1A). Hydrodynamic size of LP-THP and SP-THP was 8.2 nm and 25.9 nm respectively in aqueous solution (Fig. 1B). The larger hydrodynamic size of SP-THP was also confirmed by the size exclusion chromatography (Fig. 1C). These results clearly showed that SP-THP behaved much larger size than LP-THP in aqueous solution.

Molecular size of drugs has great impact on pharmacokinetics property and therapeutic effect [21, 22]. Most of small hydrophilic or hydrophobic molecules are quickly distributed in a whole body, and less accumulation of drugs could be observed in tumor or other lesions. In contrast, macromolecular drugs are retained longer in the systemic circulation, and they efficiently accumulate in the tumor tissue by the EPR effect. Moreover, macromolecules with larger size will accumulate more in the tumor tissue, rather than the macromolecules with smaller size [21, 22]. Therefore, pharmacokinetics of macromolecular drugs can be improved by increasing the size of macromolecular drugs. PHPMA modification of PAMAM dendrimer resulted in high-MW star-like PHPMA-based (SP) carrier (approx. 400 kDa) with narrow distribution, whereas LP-THP has MW of about 39kDa. In our previous study, DOX conjugated with SP (SP-DOX) exhibited better tumor accumulation and therapeutic effect than DOX conjugated with linear PHPMA (LP-DOX) in subcutaneous mice EL4 T-cell lymphoma model, indicating that SP carrier is preferable carrier for antitumor drugs to deliver them to the tumor tissue more efficiently [5, 6]. Recently we also showed that LP-THP exhibited the remarkable antitumor activity against S-180 subcutaneous tumor model [17].

Here we compared the antitumor activity of LP-THP and SP-THP in S-180 ectopically implanted tumor model and chemical AOM/DSS induced autochthonous tumor model.

Because of a larger size of SP-THP (25.9 nm, 400 kDa) in contrast to LP-THP (8.6 nm, 39 kDa), we anticipated that SP-THP would exhibit better pharmacokinetics, and thus antitumor effect. In S-180 tumor bearing mice, both LP-THP and SP-THP exhibited far preferable pharmacokinetic property than the conventional free THP. When we compared the LP-THP and SP-THP, tumor $AUC_{(total\ THP;\ 5h \sim 72h)}$ and $AUC_{(released\ free\ THP;\ 5h \sim 72h)}$ of SP-THP were 2.7 and 3.3 times higher than those of LP-THP respectively. More importantly, accumulation of released free THP (cytotoxic active drug) was only seen in the tumor tissue, especially 24 h after drug administration and not in any other normal organs (Fig. 4B). The data given above clearly showed that SP-THP was more selective toward tumor tissue. Because of higher tumor concentration of SP-THP, only single i.v. injection of 5 mg/kg THP equivalent dose of SP-THP was enough to suppress S-180 tumor growth completely; LP-THP and conventional free THP suppressed the tumor growth, however, the tumor gradually regrew. Antitumor activity of SP-THP was also examined using the chemical induced authocutonous tumor model. I.p. administration of AOM followed by p.o. administration of DSS causes colorectal tumor. This chemically induced tumor is more realistic tumor than ectopically inoculated tumor model, and it is difficult to treat. In such model, a single injection, however, of both conventional free THP and LP-THP could not suppress the tumor growth. In the case of SP-THP, dose of 15 mg/kg THP equivalent clearly suppressed the tumor growth; number of tumor nodule and tumor area was significantly decreased (Fig. 6). Unfortunately, slight body weight loss was seen (~15 %) in the SP-THP administration group (S. Fig 2), however, no mice died. This might be because of released free THP in the systemic circulation, which would exert adverse effect. However, LD_{50} of parent free THP, LP-THP, and SP-THP were 14.2 mg/kg, 60 mg/kg, 23.4 mg/kg, respectively (S. Table 31). Both LP-TH and SP-THP conjugate showed lower toxicity and higher therapeutic efficacy than parent free THP (Fig. 5, S. Fig 3). When both polymer THP conjugates were compared, SP-THP showed more potent toxicity (2 – 3 times) than LP-THP, indicating narrower therapeutic window. Although, the therapeutic efficacy of SP-THP was significantly higher than that of LP-THP, ultimate choice that which is better between the two for the clinical application is difficult, until the dose-limiting toxicity is clarified.